

## Anthropogenic global warming from the perspective of the Phanerozoic evolution of Earth's climate

Hubert Wierzbowski<sup>1</sup>



*Abstract.* The paper presents an overview of published data on the Phanerozoic evolution of Earth's climate, and on examples of abrupt climate warming linked to greenhouse gas emissions. A major role of carbon dioxide in long-term climate forcing is documented by the co-occurrence of geological proxies of an elevated atmospheric CO<sub>2</sub> level and high surface temperatures during the Phanerozoic history of the Earth, which is related to global geochemical processes. The rapid climatic warming during the Early Toarcian (Jurassic) and the Paleocene-Eocene transition (Paleogene) was caused by emission of greenhouse gases (CO<sub>2</sub> and CH<sub>4</sub>) from magmatic sources, thermal decomposition of fossil organic matter and their expulsion in secondary trigger processes from terrestrial and marine pools. The same phenomena are among the presumed effects of burning of fossil fuels by recent human activity. The expected anthropogenic global warming due to the combustion of the fossil fuel reserve is lesser than the major warming of the past; however, it can cause a significant increase in atmospheric CO<sub>2</sub> level and a rise in surface temperatures marking the end of the present icehouse conditions of the Earth's climate.

**Keywords:** greenhouse and icehouse climate, greenhouse gases, global geochemical processes, rapid warming episodes

### INTRODUCTION

Discussions among geologists commonly concern the role of natural climatic factors on the Earth's climate forcing. In addition, major climate changes of the past, which are recorded in geological archives, are often evaluated in terms of their comparison to recent anthropogenic warming in order to predict possible changes in the future Earth's environment. This can be done assuming constancy of long-lasting geological, geochemical or astronomical processes.

The palaeoclimatic proxies are indeed an important and sometimes underestimated source of information on the temporal and spatial variations of the Earth's climate, its long-term evolution and the influence of certain physical or chemical processes on average surface temperatures. They can also help to distinguish between present-day natural and anthropogenic factors affecting global climate. This is particularly important for predicting the longer-term effects of anthropogenic global warming and the probable length of the future recovery of the global climate to pre-industrial conditions, both of which are difficult to model. An effective approach to past climate change requires, however, that all the forcing processes and the very long Phanerozoic evolution of Earth's climate be taken into account.

### MODES OF PHANEROZOIC CLIMATE AND THEIR CO<sub>2</sub> FORCING

Two different modes of the Earth's climate in the Phanerozoic are related to the presence or absence of continental glaciation in polar regions. During greenhouse periods, high surface temperatures did not favour formation of continental ice sheets at high latitudes. This was associated with a smaller latitudinal temperature gradient, a more balanced

configuration of climatic zones and the presence of warm deep ocean water masses (cf. Crowley, Zachos, 2000; Gröcke, 2009; Zhang *et al.*, 2019 and references therein). A side-effect of the lack of continental glaciation, amplified by the presumed high activity of the oceanic crust during at last some greenhouse periods, was a high sea-level. This led to the formation of extensive, warm epeiric seas, in which shallow-water organisms flourished.

Low temperatures in the high latitudes during icehouse periods favoured formation of continental ice caps, which retained huge amounts of fresh water. This led to sea-level fall, the circulation of cold deep ocean water masses that formed in polar regions, and reduction in marine biodiversity, especially at high latitudes and in the pelagic realm (cf. Thomas, 2008; Link, 2009; Zhang *et al.*, 2019 and references therein). From a palaeoclimatic point of view the most important features of the icehouse climate are probably the enhanced latitudinal temperature gradient and the susceptibility of the high latitude climate to orbital forcing, which resulted in a cyclical pattern of transitions from glacial to interglacial in subpolar regions and, to some degree, in northern parts of middle latitudes (cf. Pailard, 2006).

The early-middle Paleozoic (except for the Late Ordovician–Early Silurian) and the Mesozoic are considered as typical greenhouse periods. The Mesozoic greenhouse climate, despite the possible occurrence of short-term cold snaps, is well-documented by the widespread distribution of thermophilic floras and faunas, specific facies patterns, including the paucity of ice-related deposits, and palaeotemperature estimates based on isotope proxies (e.g., Hallam, 1994; Sellwood, Price, 1994; Price, 1999; Rees *et al.*, 2000; Leinfelder *et al.*, 2002; Sellwood, Valdes, 2006; Fletcher *et al.*, 2008; Scotese *et al.*, 2021). During the Cenozoic a gradual switch to an icehouse climate occurred. This is well-documented by the oxygen isotope record of benthic

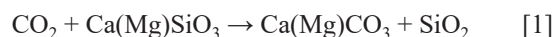
<sup>1</sup> Polish Geological Institute – National Research Institute, Rakowiecka 4, 00-975, Warsaw, Poland; e-mail: [hwier@pgi.gov.pl](mailto:hwier@pgi.gov.pl); ORCID ID: 0000-0003-2682-2945

foraminifera showing strong shifts to more positive  $\delta^{18}\text{O}$  values in the lower-middle Oligocene and, after a short-term recovery, starting from the middle Miocene onwards (Zachos *et al.*, 2001; Cramer *et al.*, 2011; Mudelsee *et al.*, 2014; Zhang *et al.*, 2019). The  $\delta^{18}\text{O}$  shifts are attributed to a combined effect of a decrease in deep-sea temperatures and an increase in continental ice-volume, first in Antarctic and then in the Northern Hemisphere. However, the Cenozoic Antarctic glaciation was additionally stimulated by the circumpolar position of this continent and its isolation, starting from the Miocene, as a result of the full opening of the Drake Passage and the formation of Antarctic Circumpolar Current (cf. Zhang *et al.*, 2010).

Geological proxies recorded in geochemical and palaeobotanical archives show a close correspondence of high surface temperatures, typical of greenhouse periods with elevated atmospheric  $\text{CO}_2$  levels (>1000 ppm) during the Phanerozoic (Pearson, Palmer, 2000; Retallack, 2002; Royer *et al.*, 2004; Royer, 2006; Glikson, 2008; Mills *et al.*, 2019; Judd *et al.*, 2024; Fig. 1). In addition, results of geochemical cycle modelling show distinct correlation of the well-documented greenhouse periods of the Phanerozoic era with high concentrations of  $\text{CO}_2$ , which is regarded as a powerful and long-lived greenhouse gas (Berner, 1991, 1994, 2006; Berner, Kothoval, 2001). Primary drivers of the Phanerozoic  $\text{CO}_2$  level and the global climate are identified as: (1) an increased rate of chemical weathering of land areas and high organic matter burial due to a rise of vascular plants starting from the Devonian, which culminated in the formation of large Carboniferous coal deposits and (2) an increased rate of silicate weathering in the Cenozoic, after the Mesozoic standstill. Both processes resulted in a distinct drop in the late Carboniferous-Permian and late Paleogene-Neogene atmospheric  $\text{CO}_2$  levels leading to icehouse conditions and continental glaciations (Royer, 2006). Comparable results, indicating slightly lower Mesozoic  $\text{CO}_2$  levels, being 3 to 7 times higher than the present one, have also been obtained using the carbon-oxygen-phosphorus-sulphur cycling model of Bergman *et al.* (2004), which neglects direct modelling of the erosion rate.

In this context, the cause of the Late Ordovician–Early Silurian glaciation occurring under inferred high  $\text{CO}_2$  level remains unclear due to the lack of precise palaeoclimatic data. It may have been facilitated by the circumpolar position of Gondwana, which made the Earth system sensitive to brief drops in atmospheric  $\text{CO}_2$  unrecorded in the sedimentary archive (cf. Gibbs *et al.*, 2000; Lv *et al.*, 2022). On the other hand, there is no proof for continental glaciation during other brief Mesozoic cold snaps as those of the early Middle Jurassic or Jurassic/Cretaceous transition (cf. Price, 1999; Scotese *et al.*, 2021). Therefore, they seem to be of regional importance only.

The long-term process of organic matter burial and of the formation of organic matter-rich deposits is generally well-known. It might have been partially reversed by natural weathering and magmatic processes, or by present-day human activity involving combustion of fossil fuels. Silicate weathering, which is the most efficient geological process of  $\text{CO}_2$  sequestration, has relied on the liberation of calcium and magnesium from igneous rocks over the whole Phanerozoic history of the Earth and the formation of thick and relatively weathering-resistant carbonate deposits. This process may be represented by the following chemical formula involving  $\text{CO}_2$  binding:



The increased rate of Cenozoic silicate weathering is usually regarded as resulting from the uplift of Himalayas or the arrival of the weathering-prone basaltic Deccan Traps in the equatorial humid belt, both of which occurred 45–50 million years ago (Retallack, 2002; Kent, Muttoni, 2013). Further acceleration of the silicate weathering during the Cenozoic may be linked to the emplacement of the Ethiopian Traps near the equator, magmatic extrusions in SE Asia and the glacial weathering of Antarctic rocks (Kent, Muttoni, 2013; Stoll *et al.*, 2024). A passage from the low rate of continental erosion during the Mesozoic to the gradually increasing rate of the continental erosion during the Cenozoic is reflected in the seawater  $^{87}\text{Sr}/^{86}\text{Sr}$  ratio. This ratio is affected by inputs of

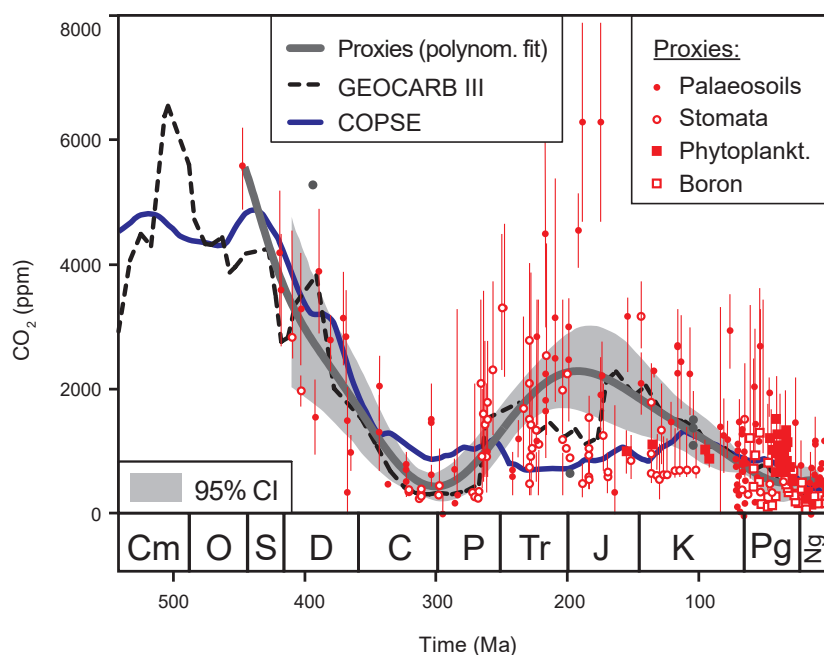


**Fig. 1.** Atmospheric  $\text{CO}_2$  concentrations during the Phanerozoic estimated on the basis of geochemical modelling i.e. the GEOCARB III model of Berner and Kothavala (2001) and the COPSE model of Bergman *et al.* (2004) as well as direct determinations of proxies for ancient  $\text{CO}_2$  level according to the database of Royer *et al.* (2004), which comprises  $\text{CO}_2$  estimates based on interpretation of  $\delta^{13}\text{C}$  values of the carbonate fraction of palaeosoils, stomatal density of plants, long-chained alkenones of haptophytic algae and  $\delta^{11}\text{B}$  values of marine carbonate fossils. A tenth degree polynomial function has been fitted to proxy data ( $R = 0.69$ ), with given 95% confidence limits (CI), to show a general trend of observed Phanerozoic  $\text{CO}_2$  variations. Customary labels of the geological periods of the Phanerozoic era and the time scale are marked at the bottom of the diagram

strontium derived from global oceanic and continental pools characterized, respectively, by low and high strontium isotope ratios (Wierzbowski, 2013). Jurassic and Early Cretaceous seawater was characterized by a low  $^{87}\text{Sr}/^{86}\text{Sr}$  ratio, with the Phanerozoic minimum of  $\sim 0.70683$  falling close to the Middle–Late Jurassic transition (Wierzbowski *et al.*, 2017; McArthur *et al.*, 2020). A general rise of  $^{87}\text{Sr}/^{86}\text{Sr}$  ratio, interrupted by a slight Paleocene–Eocene decrease, commenced in the Late Cretaceous (Coniacian; McArthur *et al.*, 2020). It culminated in the high present day seawater  $^{87}\text{Sr}/^{86}\text{Sr}$  ratio of 0.70917 (cf. El Meknassi *et al.*, 2020).

Under the low  $\text{CO}_2$  levels (<500 ppm), typical of the late Cenozoic icehouse, high latitudes became susceptible to climatic forcing linked to Milankovitch cycles (cf. Pearson, Palmer, 2000; Royer, 2006). A predominant  $\sim 100$  Ka cyclicality related to orbital eccentricity is found to affect Quaternary climate. Although, the role of eccentricity changes in the summer insolation of high latitudes is insignificant in itself, the presence of an additional mechanism of glacial dust formation, which reduces the albedo of ice, likely played a major role in the 100 Ka cyclicality of build-up and loss of

Quaternary continental ice sheets (Ganopolski, Calov, 2011; Ganopolski, Brovkin, 2017). The glacial-interglacial cycles coincide with variations in surface temperatures, deep ocean temperatures, and fluctuations in  $\delta^{18}\text{O}$  values of seawater related to the periodical increases and decreases in ice volume. These parameters are recorded in the oxygen isotope values of carbonate oozes from oceanic cores as well as the oxygen and deuterium isotope profiles of Antarctic and Greenland ice cores (cf. Petit *et al.*, 1999; Shackleton, 2000; Glikson, 2008; Lüthi *et al.*, 2008 and references therein; Fig. 2). Interestingly, the orbitally controlled temperature oscillations of the middle Pleistocene–Holocene interact with similar in-phase variations in the atmospheric  $\text{CO}_2$  level deciphered from ice-cores (Fig. 2). Although the coupling of ice sheets and carbon cycle remained, for a long time, unclear and was a source of confusion regarding the role of  $\text{CO}_2$  in the Quaternary climate forcing, recent models, which take into account physical ocean-atmosphere interactions, simulate well the magnitude and timing of glacial-interglacial atmospheric  $\text{CO}_2$  fluctuations (Ganopolski, Brovkin, 2017; Ganopolski, 2024). Only minor long-term temporal changes

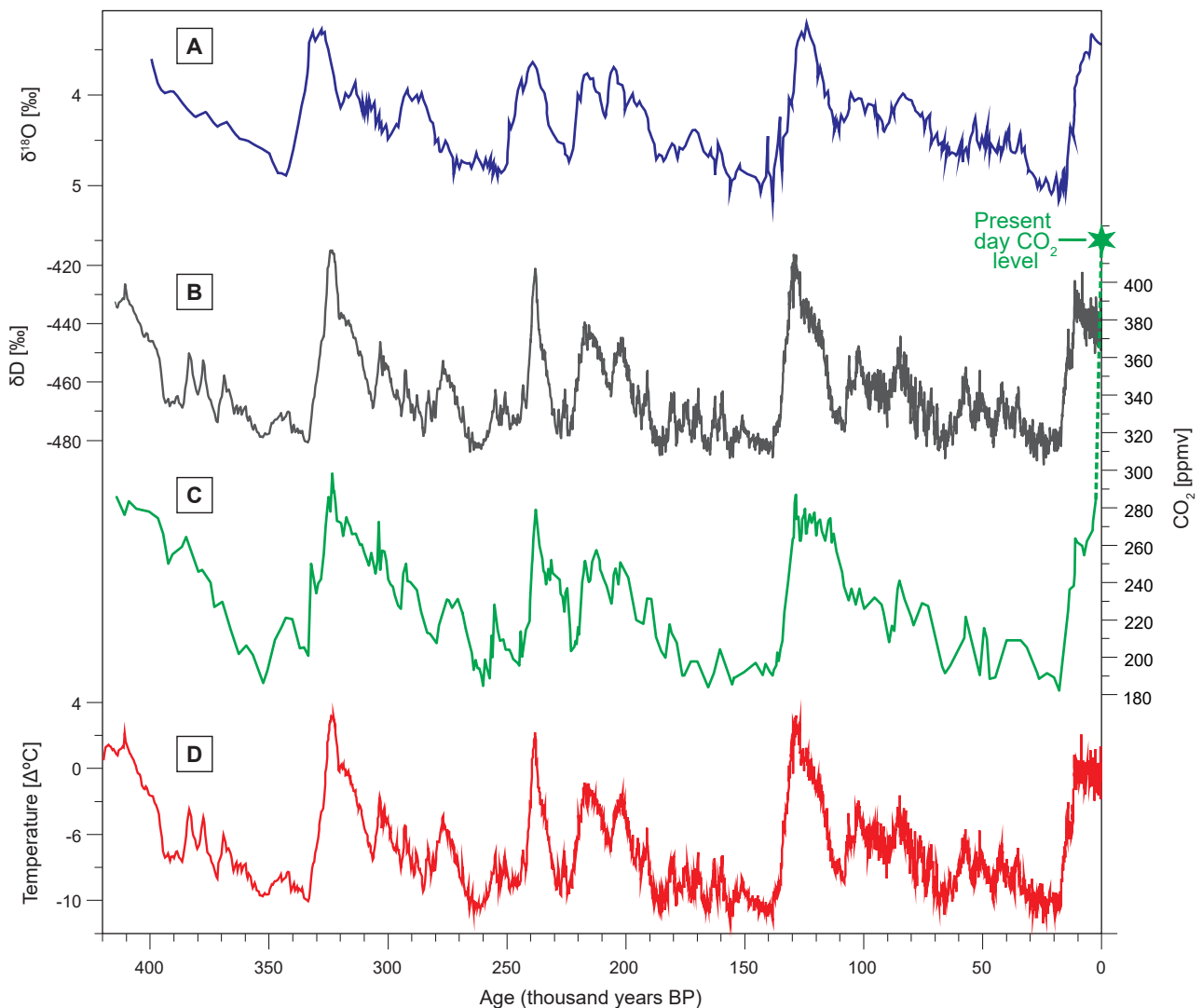


**Fig. 2.** Climatic proxies of the middle Pleistocene–Holocene. **A** – benthic  $\delta^{18}\text{O}_{\text{carbonate}}$  curve from oceanic cores V19-30 and V19-28 according to Shackleton (2000). **B** – deuterium isotope profile of the Vostok core after Petit *et al.* (1999). **C** – variations in  $\text{CO}_2$  concentrations in air bubbles of the Vostok core (solid line; after Petit *et al.*, 1999) supplemented with an industrial-era increase in atmospheric  $\text{CO}_2$  content (dashed line); the present-day atmospheric  $\text{CO}_2$  concentration is marked with asterisk. **D** – temperature variations estimated based on the  $\delta\text{D}$  signal of the Vostok core (after Petit *et al.*, 2001)

in atmospheric CO<sub>2</sub> concentrations of the last 800 Ka may represent a feedback of the Earth system to variations in the global weathering rate (Lüthi *et al.*, 2008).

Notably, human activity is resulting in a rapid increase in atmospheric CO<sub>2</sub> level. Its present-day value (425 ppm) significantly exceeds the pre-industrial atmospheric CO<sub>2</sub> concentration (280 ppm), which is close to the maxima of the past four interglacial ages recorded in ice-cores (Fig. 2). It brings Earth's climate closer and closer to the so-called "cool non-glacial conditions" predicted for the CO<sub>2</sub> range between 500 and 1000 ppm (Royer, 2006). The question arises as to whether similar rapid climatic phenomena occurred in the geological history of the Earth and whether the past natural climate change may be used as a key for the interpretation of the present anthropogenic one.

### RAPID WARMING EVENTS IN THE PHANEROZOIC

Severe climate changes occurred during the Phanerozoic history of the Earth. These were mostly linked to perturbations in the global carbon cycle, which are recorded in the  $\delta^{13}\text{C}$  values of marine carbonates as well as the  $\delta^{13}\text{C}$  values of marine and terrestrial organic matter. A significant role of rapid greenhouse gas emissions, caused by volcanic processes, and its impact on the Mesozoic-Cenozoic Earth's climate is well-studied and discussed as regards the Permian-Triassic mass extinction event (PTME) end-Triassic mass extinction (ETE), early Toarcian Oceanic Anoxic Event (TOAE), early Aptian Selli Event (or OAE 1a), Cenomanian-Turonian boundary Bonarelli event (or OAE2), Cretaceous-Paleogene (K-Pg) extinction event, Paleocene-Eocene thermal maximum (PETM) and the Eocene Thermal Maximum 2 (ETM-2). The course of geological phenomena responsible for the emergence of these events has been reviewed in detail (e.g., Keller *et al.*, 2011; Davies *et al.*, 2017; Remírez, Algeo, 2020; Joo *et al.*, 2020; Harper *et al.*, 2020; Hull *et al.*, 2020; Kender *et al.*, 2021; Dal Corso *et al.*, 2022; Jiang *et al.*, 2022 and references therein). From the point of view of anthropogenic global warming, the well-studied "supergreenhouse" episodes of the Early Jurassic TOAE (also called the "Jenkyns Event") and the Paleocene-Eocene PETM are particularly interesting. Both episodes are considered as related to emissions of CO<sub>2</sub> and CH<sub>4</sub> gases that are well-recorded in sedimentary archives. They resulted in strong perturbations of the global carbon cycle and global warming.

#### Toarcian Oceanic Anoxic Event

Formation of the large Karroo-Ferrar igneous province (~183 million years ago) located in the southern Gondwana resulted in huge magmatic CO<sub>2</sub> and thermogenic CH<sub>4</sub> and CO<sub>2</sub> emissions in short-term pulses that are responsible for the TOAE (Ivanov *et al.*, 2017; Font *et al.*, 2022). Emission of thermogenic gases has been linked to the intrusion of Karroo-Ferrar sills into organic-rich sedimentary host rocks containing coal deposits. This process may be compared to the combustion of fossil fuels. The TOAE occurred after the Late Pliensbachian cooling event (Korte, Hesselbo, 2011; Gómez *et al.*, 2016). Processes involved in the amplification of greenhouse forcing, which were triggered by rising surface temperatures, likely included dissociation of shallow-marine methane clathrates and decomposition of terrestrial organic matter (Jenkyns, 1988; Hesselbo *et al.*, 2000; Pieńkowski *et al.*, 2016).

The emission of greenhouse gases is recorded worldwide by a negative carbon isotope excursion in the lower part of the Falciferum (Serpentinum) Zone of the Lower Toarcian, which is characterized by 6–7 and ~2‰ negative shifts in organic matter and marine carbonate  $\delta^{13}\text{C}$  values, respectively (e.g., Hesselbo *et al.*, 2000, 2007; Kemp *et al.*, 2011; Hermoso *et al.*, 2012; Suan *et al.*, 2015; Arabas *et al.*, 2017; Them II *et al.*, 2017; Xu *et al.*, 2018; Boulila *et al.*, 2019; Reolid *et al.*, 2020; Fig. 3). The negative excursion is also documented in the Polish Basin (Hessebo, Pieńkowski, 2011; Pieńkowski *et al.*, 2016, 2020). It was accompanied by global warming of 6–8°C inferred from isotopic and chemical proxies, a crisis of carbonate productivity and a marine extinction event linked to ocean acidification (Bailey *et al.*, 2003; Suan *et al.*, 2010; Gómez, Goy, 2011; Caruthers *et al.*, 2013; Krencker *et al.*, 2020). The global warming and freshening of Arctic surface seawaters likely led to the slowdown of global oceanic circulation, ocean stratification, and bottom water anoxia, which is manifested by the widespread occurrences of black shales (Dera, Donnadieu, 2012; Remírez, Algeo, 2020). An increase in *p*CO<sub>2</sub> level, from the latest Pliensbachian ~850 to ~1750 ppm during the pre-TOAE, is suggested based on botanical and geochemical proxies (McElwain *et al.*, 2005; Müller *et al.*, 2020). The emission of greenhouse gases during the TOAE, mostly in the form of CH<sub>4</sub>, has been variously estimated in different studies, from 1500–2700 Gt of pure carbon by Hesselbo *et al.* (2000), to 10,000 Gt of carbon by McElwain *et al.* (2005) and 15,000–27,000 Gt of carbon in more recent papers (cf. Suan *et al.*, 2015; Remírez, Algeo, 2020). The absolute timing of TOAE is, up to now, poorly constrained. Although most astrochronological calibration suggests its 300–500 Ka duration and the high-frequency carbon cycle oscillations during its initial part (Boulila *et al.*, 2014, 2019; Boulila, Hinnov, 2017) the duration of TOAE has been estimated at up to ~900 Ka by other authors (cf. Huang, Hesselbo, 2014; Pieńkowski *et al.*, 2024).

#### Paleocene-Eocene Thermal Maximum

PETM is a well-known greenhouse episode, which occurred ~55,6 Ma ago at the Paleocene-Eocene transition. It is marked by a few permil negative  $\delta^{13}\text{C}$  excursion, mostly related to emission of magmatic and thermogenic gases during the formation of the North Atlantic Igneous Province, albeit evidence for this scenario is ambiguous (Svensen *et al.*, 2004; Storey *et al.*, 2007; Gutjahr *et al.*, 2017; Kender *et al.*, 2021). Therefore, the carbon isotope excursion has also been related to the emission of CH<sub>4</sub> and CO<sub>2</sub> from secondary carbon reservoirs, i.e. dissociation of marine methane clathrates or a decay of terrestrial organic matter in response to an initial warming caused by magmatic processes (Dickens *et al.*, 1995; Matsumoto, 1995; Kurtz *et al.*, 2003; DeConto *et al.*, 2012; Kender *et al.*, 2021) or linked to a bolid impact (Kent *et al.*, 2003; Cramer and Kent, 2005; Schaller *et al.*, 2016).

The estimations of a global temperature rise during the PETM range from 3 to 8°C but most of them oscillate between 4 and 5°C (Sluijs and Brinkhuis, 2008; McInerney and Wing, 2011; Dunkley Jones *et al.*, 2013; Evans *et al.*, 2016). The duration of the onset of PETM, comprising a decrease to minimal  $\delta^{13}\text{C}$  values, has been variously calculated from 750 years to 30 Ka (Röhl *et al.*, 2007; Murphy *et al.*, 2010; Wright and Schaller, 2013; Turner, Ridgwell, 2016). Recent astronomical calibration, however, suggests a 6 Ka duration of its onset (Li *et al.*, 2022). The time span

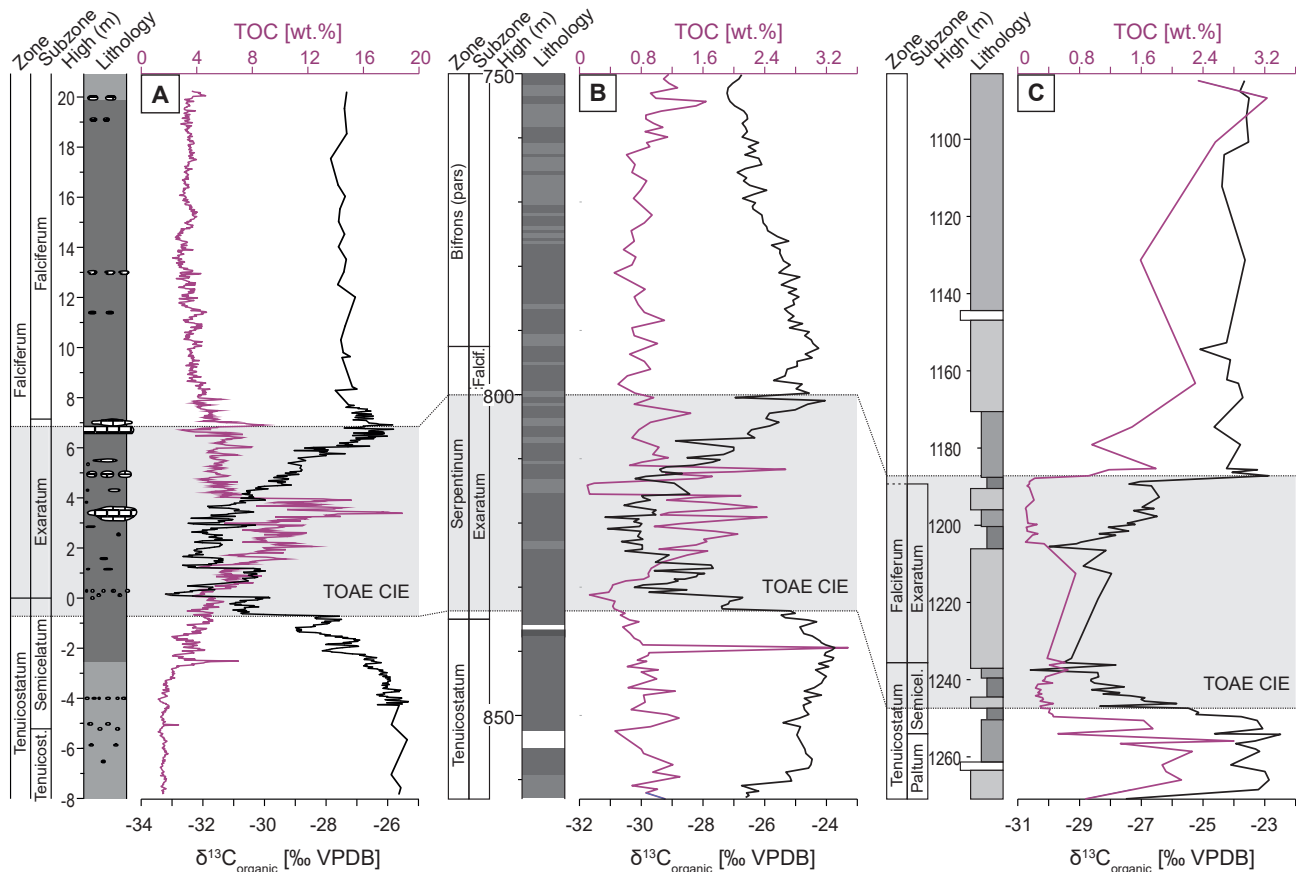


**Fig. 3.** Organic matter carbon isotope variations and total organic carbon (TOC) values of bulk sediments at the interval of the carbon isotope excursion (CIE) associated with the TOAE. **A** – Whitby section, Yorkshire, UK (after Kemp *et al.*, 2011). **B** – Mochras borehole, Wales, UK (after Xu *et al.*, 2018; Pieńkowski *et al.*, 2024). **C** – Kaszewy borehole, central Poland (after Pieńkowski *et al.*, 2020). The TOAE CIE excursion is marked in light grey. A lack of TOC enrichment in the CIE interval of the Kaszewy section is likely due to the shallowness of the Polish basin, which resulted in a lack of anoxic conditions and in decay of labile marine organic matter that predominated during this interval (Pieńkowski *et al.*, 2016, 2020).

of the entire PETM event from the onset until its termination and a return to cooler climatic conditions, similar to those of pre-PETM, is calculated at 170 Ka and includes a ~80 Ka period of the recovery phase (Röhl *et al.*, 2007; Murphy *et al.*, 2010; Wright, Schaller, 2013). The PETM timing constrains the assumptions of palaeoclimatic models but due to its rapid onset this event is often regarded as caused by a burst of greenhouse gas emission.

The modelling of carbon cycle perturbations during the PETM suggest a total emission of 3,000 to 17,000 Gt carbon, which may have included emissions by secondary, trigger processes (Zeebe *et al.*, 2009; Cui *et al.*, 2011; Wright, Schaller, 2013; Meissner *et al.*, 2014). The emission may have doubled the initial atmospheric CO<sub>2</sub> level of 800–1700 ppm (Zeebe *et al.*, 2009; Meissner *et al.*, 2014). Interestingly, the methane scenario of PETM imposes a lower peak level of *p*CO<sub>2</sub> of ~1200 ppm (Cui, Schubert, 2017). However, some calculations of carbon emission during the PETM may be underestimated due to the relatively heavy carbon isotope signatures of volcanogenic CO<sub>2</sub> gas, which hampers proper assessment of its amount (Gutjahr *et al.*, 2017).

## CONCLUSIONS

This short review of palaeoclimatic data on the evolution of Earth's climate during the Phanerozoic and concerning abrupt warming episodes bring us to the conclusion that its

primary drivers are greenhouse gases. Their link with long-term climatic variations and rapid warming episodes may be deciphered from geochemical archives of past sea-surface temperatures, perturbations in the global carbon cycle and ancient atmospheric *p*CO<sub>2</sub> levels. Importantly, the brief greenhouse episodes of the past, including the TOAE and PETM, show many similarities with the already initiated anthropogenic global warming. This applies to both the expected effects of rapid emissions of greenhouse gases on surface temperatures and their geochemical record in the form of negative carbon isotope excursions, which can be compared to the present-day isotope Suess effect (cf. Keeling, 1979; Eide *et al.*, 2017).

Recent estimates of carbon emissions during the major supergreenhouse episodes of the past, including the TOAE and PETM, exceed expected anthropogenic emissions (4600–4800 Gt of carbon) caused by burning of the known global fossil fuel reserves (cf. Glikson, 2008; Parker, Mainelli, 2024). However, this anthropogenic process will have significant impact on the global climate, and may result in a considerable increase in atmospheric CO<sub>2</sub>, even >1000 ppm, to cause major global warming (cf. Parker, Mainelli, 2024). Although it is difficult to project melting of the entire Antarctica ice-cap under future global warming, due to the specific position of this continent in a circumpolar region with elevation of many parts of its interior (cf. O'Donnell, Nyblade, 2014) the process of the glaciostatic sea-level rise, even below the maximum of 60–70 m, will have significant impact on humankind.

Climatic models take into account ~300 Gt of carbon emitted since the beginning of the industrial age but there is still insufficient data to estimate the full size and speed of the expected warming. Secondary emissions from terrestrial and marine sources, which can be released by trigger processes, are additionally difficult to calculate. The rate of future global warming will, however, depend on the rate of world-wide annual anthropogenic CO<sub>2</sub> emissions, presently calculated at 10 Gt of carbon per year (Le Quéré *et al.*, 2018; Friedlingstein *et al.*, in press).

**Acknowledgments.** Krzysztof Ninard is thanked for an insightful review and suggested amendments to the manuscript.

## REFERENCES

- ARABAS A., SCHLÖGL J., MEISTER C. 2017 – Early Jurassic carbon and oxygen isotope records and seawater temperature variations: insights from marine carbonate and belemnite rostra (Pieniny Klippen Belt, Carpathians). *Palaeogeography, Palaeoclimatology, Palaeoecology*, 485: 119–135.
- BAILEY T.R., ROSENTHAL Y., MCARTHUR J.M., VAN DO SCHOOTBRUGGE B., THIRLWALL M.F. 2003 – Paleooceanographic changes of the Late Pliensbachian–Early Toarcian interval: a possible link to the genesis of an Oceanic Anoxic Event. *Earth and Planetary Science Letters*, 212: 307–320.
- BERGMAN N.M., LENTON T.M., WATSON A.J. 2004 – COPSE: a new model of biogeochemical cycling over Phanerozoic time. *American Journal of Science*, 304: 397–437.
- BERNER R.A. 1991 – A model for atmospheric CO<sub>2</sub> over Phanerozoic time. *American Journal of Science*, 291: 339–376.
- BERNER R.A. 1994 – GEOCARB II: a revised model of atmospheric CO<sub>2</sub> over Phanerozoic time. *American Journal of Science*, 294: 56–91.
- BERNER R.A. 2006 – GEOCARBSULF: a combined model for Phanerozoic atmospheric O<sub>2</sub> and CO<sub>2</sub>. *Geochimica et Cosmochimica Acta*, 70: 5653–5664.
- BERNER R.A., KOTHOVALA Z. 2001 – GEOCARB III: a revised model of atmospheric CO<sub>2</sub> over Phanerozoic time. *American Journal of Science*, 301: 182–204.
- BOULILA S., GALBRUN B., HURET E., HINNOV L.A., ROUGET I., GARDIN S., BARTOLINI A. 2014 – Astronomical calibration of the Toarcian Stage: implications for sequence stratigraphy and duration of the early Toarcian OAE. *Earth and Planetary Science Letters*, 386: 98–111.
- BOULILA S., HINNOV L.A. 2017 – A review of tempo and scale of the early Jurassic Toarcian OAE: implications for carbon cycle and sea level variations. *Newsletters on Stratigraphy*, 50: 363–389.
- BOULILA S., GALBRUN B., SADKI D., GARDIN S., BARTOLINI A. 2019 – Constraints on the duration of the early Toarcian T-OAE and evidence for carbon-reservoir change from the High Atlas (Morocco). *Global and Planetary Change*, 175: 113–128.
- CARUTHERS A.H., SMITH P.L., GRÖCKE D.R. 2013 – The Pliensbachian–Toarcian (Early Jurassic) extinction, a global multi-phase event. *Palaeogeography, Palaeoclimatology, Palaeoecology*, 386: 104–118.
- CRAMER B.S., KENT D.V. 2005 – Bolide summer: the Paleocene/Eocene thermal maximum as a response to an extraterrestrial trigger. *Palaeogeography, Palaeoclimatology, Palaeoecology*, 224: 144–166.
- CRAMER B.S., MILLER K.G., BARETT P.J., WRIGHT J.D. 2011 – Late Cretaceous–Neogene trends in deep ocean temperature and continental ice volume: reconciling records of benthic foraminiferal geochemistry ( $\delta^{18}\text{O}$  and Mg/Ca) with sea level history. *Journal of Geophysical Research*, 116, C12023.
- CROWLEY T.J., ZACHOS J.C. 2000 – Comparison of zonal temperature profiles for past warm time periods. [In:] Huber B.T., MacLeod K.G., Wing S.L. (eds.), *Warm Climates in Earth History*. Cambridge University Press: 50–76.
- CUI Y., SCHUBERT B.A. 2017 – Atmospheric *p*CO<sub>2</sub> reconstructed across five early Eocene global warming events. *Earth and Planetary Science Letters*, 478: 225–233.
- CUI Y., KUMPL R., RIDGWELL A.J., CHARLES A.J., JUNIUM C.K., DIEFENDORF A.F., FREEMAN K.H., URBAN N.M., HARDING I.C. 2011 – Slow release of fossil carbon during the Paleocene–Eocene Thermal Maximum. *Nature Geoscience*, 4: 481–485.
- DAL CORSO J., SONG H., CALLEGARO S., CHU D., SUN Y., HILTON J., GRASBY S.E., JOACHIMSKI M.M., WIGNALL P.B. 2022 – Environmental crises at the Permian–Triassic mass extinction. *Nature Reviews Earth and Environment*, 3: 197–214.
- DAVIES J.H.F.L., MARZOLI A., BERTRAND H., YUBI N., ERNESTO M., SCHALTEGGER U. 2017 – End-Triassic mass extinction started by intrusive CAMP activity. *Nature Communications*, 8, 15596.
- DECONTO R.M., GALEOTTI S., PAGANI M., TRACY D., SCHAEFER K., ZHANG T., POLLARD D., BEERLING D.J. 2012 – Past extreme warming events linked to massive carbon release from thawing permafrost. *Nature*, 484: 87–91.
- DERA G., DONNADIEU Y. 2012 – Modeling evidences for global warming, Arctic seawater freshening, and sluggish oceanic circulation during the Early Toarcian anoxic event. *Paleoceanography*, 27, PA2211.
- DICKENS G.R., O'NEIL J.R., REA D.K., OWEN R.M. 1995 – Dissociation of oceanic methane hydrate as a cause of the carbon isotope excursion at the end of the Paleocene. *Paleoceanography*, 10: 965–971.
- DUNKLEY JONES T., LUNT D.J., SCHMIDT D.N., RIDGWELL A., SLUIJS A., VALDES P.J., MASLINE M. 2013 – Climate model and proxy data constraints on ocean warming across the Paleocene–Eocene Thermal Maximum. *Earth-Science Reviews*, 125: 123–145.
- EIDE M., OLSEN A., NINNEMANN U.S., ELDEVIK T. 2017 – A global estimate of the full oceanic <sup>13</sup>C Suess effect since the preindustrial. *Global Biogeochemical Cycles*, 31: 492–514.
- EL MEKNASSI E., DERA G., DE RAFÉLIS D., BRAHMI C., LARTAUD F., HODEL F., JEANDEL C., MENJOT L., MOUNIC S., HENRY M., BESSON P., CHAVAGNAC V. 2020 – Seawater <sup>87</sup>Sr/<sup>86</sup>Sr ratios along continental margins: patterns and processes in open and restricted shelf domains. *Chemical Geology*, 558, 119874.
- EVANS D., WADE B.S., HENEHAN M., EREZ J., MÜLLER W. 2016 – Revisiting carbonate chemistry controls on planktic foraminifera Mg/Ca: implications for sea surface temperature and hydrology shifts over the Paleocene–Eocene Thermal Maximum and Eocene–Oligocene transition. *Climate of the Past*, 12: 819–835.
- FLETCHER B.J., BRENTNALL S.J., ANDERSON C.W., BERNER R.A., BEERLING D.J. 2008 – Atmospheric carbon dioxide linked with Mesozoic and early Cenozoic climate change. *Nature Geoscience*, 11: 43–48.
- FONT E., DUARTE L.V., DEKKERS M.J., REMAZEILLES C., EGLI R., SPANGENBERG J.E., FANTASIA A., RIBEIRO J., GOMES E., MIRÃO J. 2022 – Rapid light carbon releases and increased aridity linked to Karoo–Ferrar magmatism during the early Toarcian oceanic anoxic event. *Scientific Reports*, 12, 4342.
- FRIEDLINGSTEIN P., O'SULLIVAN M., JONES M.W., ANDREW R.M., HAUCK J., LANDSCHÜTZER P., LE QUÉRE C., LI H., LUIJKX I.T., OLSEN A., PETERS G.P., PETERS W., PONGRATZ J., SCHWINGSCHACK L., SITCH S., CANADELL J.G., CIAIS P., JACKSON R.B., ALIN S.R., ARNEH A., ARORA V., BATES N.R., BECKER M., BELLOUIN N., BERGHOF C.F., BITTIG H.C., BOPP L., CADULE P., CAMPBELL K., CHAMBERLAIN M.A., CHANDRA N., CHEVALIER F., CHINI L.P., COLLIGAN T., DECAYEUX J., DJEUTCHOUANG L., DOU X., DURAN ROJAS C., ENYO K., EVANS W., FAY A., FEELY R.A., FORD D.J., FOSTER A., GASSER T., GEHLEN M., GKRTZALIS T., GRASSI G., GREGOR L., GRUBER N., GÜRSES Ö., HARRIS I., HEFNER M., HEINKE J., HURTT G.C., IIDA Y., IL-YINA T., JACOBSON A.R., JAIN A., JARNÍKOVÁ T., JERSILD A., JIANG F., JIN Z., KATO E., KEELING R.F., KLEIN GOLDEWIJK K., KNAUER J., KORSBAKKEN J.I., LAUVSET S.K., LEFÈVRE N., LIU Z., LIU J., MA L., MAKSYUTOV S., MARLAND G., MAYOT N., MCGUIRE P., METZL N., MONACCI N.M., MORGAN E.J., NAKAOKA S.-I., NEILL C., NIWA Y., NÜTZEL T., OLIVIER L., ONO T., PALMER P.I., PIERROT D., QIN Z., RESPLANDY L., ROOBAERT A., ROSAN T.M., RÖDENBECK C., SCHWINGER J., SMALLMAN T. L., SMITH S., SOSPEDRA-ALFONSO R., STEINHOFF T., SUN Q., SUTTON A.J., SÉFÉRIAN R., TAKAO S., TATEBE H., TIAN H., TILBROOK B., TORRES O., TOURIGNY E., TSUJINO H., TUBIELLO F., VAN DER WERF G., WANNINKHOF R., WANG X., YANG D., YANG X., YU Z., YUAN W., YUE X., ZAEHLE S., ZENG N., ZENG J. *et al.* (in press) – GLOBAL CARBON BUDGET 2024. *Earth System Science Data*. <https://doi.org/10.5194/essd-2024-519>
- GANOPOLSKI A. 2024 – Toward generalized Milankovitch theory (GMT). *Climate of the Past*, 20: 151–185.
- GANOPOLSKI A., BROVKIN V. 2017 – Simulation of climate, ice sheets and CO<sub>2</sub> evolution during the last four glacial cycles with an Earth system model of intermediate complexity. *Climate of the Past*, 13: 1695–1716.
- GANOPOLSKI A., CALOV R. 2011 – The role of orbital forcing, carbon dioxide and regolith in 100 kyr glacial cycles. *Climate of the Past*, 7: 1415–1425.
- GIBBS M.T., BICE K.L., BARRON E.J., KUMPL R. 2000 – Glaciation in the early Paleozoic 'greenhouse': the roles of paleogeography and atmospheric CO<sub>2</sub>. [In:] Huber B.T., MacLeod K.G., Wing S.L. (eds.), *Warm Climates in Earth History*. Cambridge University Press: 386–422.
- GLIKSON A.Y. 2008 – Milestones in the evolution of the atmosphere with reference to climate change. *Australian Journal of Earth Sciences*, 55: 125–139.

- GÓMEZ J.J., GOY A. 2011 – Warming-driven extinction in the Early Toarcian (Early Jurassic) of northern and central Spain. Correlation with other time-equivalent European sections. *Palaeogeography, Palaeoclimatology, Palaeoecology*, 306: 176–195.
- GÓMEZ J.J., COMAS-RENGIFO M.J., GOY A. 2016 – Palaeoclimatic oscillations in the Pliensbachian (Early Jurassic) of the Asturian Basin (Northern Spain). *Climate of the Past*, 12: 1199–1214.
- GRÖCKE D.R. 2009 – “Greenhouse” (warm) climates. [In:] Gornitz V. (ed.), *Encyclopedia of Palaeoclimatology and Ancient Environments*. Springer: 397–405.
- GUTJAHR M., RIDGWELL A., SEXTON P.F., ANAGNOSTOU E., PEARSON P.N., PÄLIKE H., NORRIS R.D. 2017 – Very large release of mostly volcanic carbon during the Palaeocene–Eocene Thermal Maximum. *Nature*, 548: 573–577.
- HALLAM A. 1994 – Jurassic climates as inferred from the sedimentary and fossil record. [In:] Allen J.R.L., Hoskins B.J., Sellwood B.W., Spicer R.A., Valdes P.J. (eds.), *Palaeoclimates and Their Modelling with Special Reference to the Mesozoic Era*. Chapman and Hall for the Royal Society: 79–88.
- HARPER D.T., HÖNISCH B., ZEEBE R.E., SHAFER G., HAYNES L.L., THOMAS E., ZACHOS J.C. 2020 – The magnitude of surface ocean acidification and carbon release during Eocene Thermal Maximum 2 (ETM-2) and the Paleocene-Eocene Thermal Maximum (PETM). *Paleoceanography and Paleoclimatology*, 35, e2019PA003699.
- HERMOSO M., MINOLETTI F., RICKABY S.P., HESSELBO S.P., BAUDIN F., JENKYN H.C. 2012 – Dynamic of a stepped carbon-isotope excursion: ultra high-resolution study of Early Toarcian environmental change. *Earth and Planetary Science Letters*, 319/320: 45–54.
- HESSELBO S.P., PIENKOWSKI G. 2011 – Stepwise atmospheric carbon-isotope excursion during the Toarcian Oceanic Anoxic Event (Early Jurassic, Polish Basin). *Earth and Planetary Science Letters*, 301: 365–372.
- HESSELBO S.P., GRÖCKE D.R., JENKYN H.C., BJERRUM C.J., FARRIMOND P., MORGANS BELL H.S., GREEN O.R. 2000 – Massive dissociation of gas hydrate during a Jurassic oceanic anoxic event. *Nature*, 406: 392–395.
- HESSELBO S.P., JENKYN H.C., DUARTE L.V., OLIVIEIRA L.C.V. 2007 – Carbon-isotope record of the Early Jurassic (Toarcian) Oceanic Anoxic Event from fossil wood and marine carbonate (Lusitanian Basin, Portugal). *Earth and Planetary Science Letters*, 253: 455–470.
- HUANG C., HESSELBO S.P. 2014 – Pacing of the Toarcian Oceanic Anoxic Event (Early Jurassic) from astronomical correlation of marine sections. *Gondwana Research*, 25: 1348–1356.
- HULL P.M., BORNEMANN A., PENMAN D.E., HENEHAN M.J., NORRIS R.D., WILSON P.A., BLUM P., ALEGRET L., BATENBURG S.J., BOWN P.R., BRALOWER T.J., COURNEDE C., DEUTSCH A., DONNER B., FRIEDRICH O., JEHL S., KIM H., KROON D., LIPPERT P.C., LOROCH D., MOEBIUS I., MORIYA K., PEPPE D., RAVIZZA G.E., RÖHL U., SCHUETH J.D., SEPÚLVEDA J., SEXTON P.F., SIBERT E.C., ŚLIWIŃSKA K., SUMMONS R.E., THOMAS E., WESTERHOLD T., WHITESIDE J.H., YAMAGUCHI T., ZACHOS J.C. 2020 – On impact and volcanism across the Cretaceous–Paleogene boundary. *Science*, 367: 266–272.
- IVANOV A.V., MEFFRE S., THOMPSON J., CORFU F., KAMENETSKY V.S., KAMENETSKY M.B., DEMONTEROVA E.I. 2017 – Timing and genesis of the Karoo–Ferrar large igneous province: new high precision U–Pb data for Tasmania confirm short duration of the major magmatic pulse. *Chemical Geology*, 455: 32–43.
- JENKYN H.C. 1988 – The Early Toarcian (Jurassic) anoxic event – stratigraphic, sedimentary, and geochemical evidence. *American Journal of Science*, 288: 101–151.
- JIANG Q., JOURDAN F., OLIEROOK H.K.H., MERLE R.E., BOURDET J., FOUGEROUSE D., GODEL B., WALKER A.T. 2022 – Volume and rate of volcanic CO<sub>2</sub> emissions governed the severity of past environmental crises. *Proceedings of the National Academy of Sciences*, 119, e2202039119.
- JOO Y.J., SAGEMAN B.B., HURTGEN M.T. 2020 – Data-model comparison reveals key environmental changes leading to Cenomanian–Turonian Oceanic Anoxic Event 2. *Earth-Science Reviews*, 203: 103123.
- JUDD E.J., TIERNEY J.E., LUNT D.J., MONTAÑEZ I.P., HUBER B.T., WING S.L., VALDES P.J. 2024 – A 485-million-year history of Earth’s surface temperature. *Science*, 385, eadk3705.
- KEELING C.D. 1979 – The Suess effect: <sup>13</sup>Carbon–<sup>14</sup>Carbon interrelations. *Environment International*, 2: 229–300.
- KELLER C.E., HOCHULI P.A., WEISSERT H., BERNASCONI S.M., GIORGIONI M., GARCIA T.I. 2011 – A volcanically induced climate warming and floral change preceded the onset of OAE1a (Early Cretaceous). *Palaeogeography, Palaeoclimatology, Palaeoecology*, 305: 43–49.
- KEMP D.B., COE A.L., COHEN A.S., WEEDON G.P. 2011 – Astronomical forcing and chronology of the early Toarcian (Early Jurassic) oceanic anoxic event in Yorkshire, UK. *Paleoceanography*, 26, PA4210.
- KENDER S., BOGUS K., PEDERSEN G.K., DYBKJÆR K., MATHER T.A., MARIANI E., RIDGWELL A., RIDING J.B., WAGNER T., HESSELBO S.P., LENG M.J. 2021 – Paleocene/Eocene carbon feedbacks triggered by volcanic activity. *Nature Communications*, 12, 5186.
- KENT D.V., MUTTONI G. 2013 – Modulation of Late Cretaceous and Cenozoic climate by variable drawdown of atmospheric pCO<sub>2</sub> from weathering of basaltic provinces on continents drifting through the equatorial humid belt. *Climate of the Past*, 9: 525–546.
- KENT D.V., CRAMER B.S., LANCI L., WANG D., WRIGHT J.D., VAN DER VOO R. 2003 – A case for a comet impact trigger for the Paleocene/Eocene thermal maximum and carbon isotope excursion. *Earth and Planetary Science Letters*, 211: 13–26.
- KORTE C., HESSELBO S.P. 2011 – Shallow marine carbon and oxygen isotope and elemental records indicate icehouse-greenhouse cycles during the Early Jurassic. *Paleoceanography*, 26, PA4219.
- KRENZLER F.-N., FANTASIA A., DANISCH J., MARTINDALE R., KABIRI L., EL OUALI M., BODIN S. 2020 – Two-phased collapse of the shallow-water carbonate factory during the late Pliensbachian–Toarcian driven by changing climate and enhanced continental weathering in the Northwestern Gondwana Margin. *Earth-Science Reviews*, 208, 103254.
- KURTZ A.C., KUMPL R., ARTHUR M.A., ZACHOS J.C., PAYTAN A. 2003 – Early Cenozoic decoupling of the global carbon and sulfur cycles. *Paleoceanography*, 18, 1090.
- LE QUÉRE C., ANDREW R.M., FRIEDLINGSTEIN P., SITCH S., HAUCK J., PONGRATZ J., PICKERS P.A., IVAR KORSBAKKEN J., PETERS G.P., CANADELL J.G., ARNETH A., ARORA V.K., BARBERO L., BASTOS A., BOPP L., CHEVALLIER F., CHINI L.P., CIAIS P., DONEY S.C., GKCRITZALIS T., GOLL D.S., HARRIS I., HAVERD V., HOFFMAN F.M., HOPPEMA M., HOUGHTON R.A., HURTT G., ILYINA T., JAIN A.K., JOHANNESEN T., JONES C.D., KATO E., KEELING R.F., GOLDEWIJK K.K., LANDSCHÜTZER P., LEFÈVRE N., LIENERT S., LIU Z., LOMBARDOZZI D., METZL N., MUNRO D.R., NABEL J.E.M.S., NAKAOKA S.-I., NEILL C., OLSEN A., ONO T., PATRA P., PEREGON A., PETERS W., PEYLIN P., PFEIL B., PIERROT D., POULTER B., REHDER G., RESPLANDY L., ROBERTSON E., ROCHER E.M., RÖDENBECK C., SCHUSTER U., SCHWINGER J., SÉFÉRIAN R., SKJELVAN I., STEINHOFF T., SUTTON A., TANS P.P., TIAN H., TILBROOK B., TUBIELLO F.N., VAN DER LAAN-LUIJKX I.T., VAN DER WERF G.R., VIOVY N., WALKER A.P., WILTSHIRE A.J., WRIGHT R., ZAEHLE S., ZHENG B. 2018 – Global Carbon Budget 2018. *Earth System Science Data*, 10: 2141–2194.
- LEINFELDER R.R., SCHMID D.U., NOSE M., WERNER W. 2002 – Jurassic reef patterns – the expression of a changing globe. [In:] Kiessling W., Flügel E., Golonka J. (eds.), *Phanerozoic Reef Patterns*. SEPM Special Publication, 72: 467–520.
- LI M., BRALOWER T.J., KUMPL R., SELF-TRAIL J.M., ZACHOS J.C., RUSH W.D., ROBINSON M.M. 2022 – Astrochronology of the Paleocene-Eocene Thermal Maximum on the Atlantic Coastal Plain. *Nature Communications*, 13: 5618.
- LINK P.K. 2009 – “Icehouse” (cold) climates. [In:] Gornitz V. (ed.), *Encyclopedia of Palaeoclimatology and Ancient Environments*. Springer: 463–471.
- LÜTHI D., LE FLOCH M., BEREITER B., BLUNIER T., BARNOLA J.-M., SIEGENTHALER U., RAYNAUD D., JOUZEL J., FISCHER H., KAWAMURA K., STOCKER T.F. 2008 – High-resolution carbon dioxide concentration record 650,000–800,000 years before present. *Nature*, 453: 379–382.
- LV Y., LIU S.-A., WU H., SUN Z., LI C., FAN J.X. 2022 – Enhanced organic carbon burial intensified the end-Ordovician glaciation. *Geochronology Letters*, 21: 13–17.
- MATSUMOTO R. 1995 – Causes of the δ<sup>13</sup>C anomalies of carbonates and a new paradigm ‘Gas-Hydrate Hypothesis’ (in Japanese with English summary). *Journal of the Geological Society of Japan*, 11: 902–904.
- MCARTHUR J.M., HOWARTH R.J., SHIELDS G.A., ZHOU Y. 2020 – Chapter 7 – Strontium Isotope Stratigraphy. [In:] Gradstein F.M., Ogg J.G., Schmitz M.D., Ogg G.M. (eds.), *Geologic Time Scale 2020*. Elsevier, 1: 211–238.
- MCELWAIN J.C., WADE-MURPHY J., HESSELBO S.P. 2005 – Changes in carbon dioxide during an oceanic anoxic event linked to intrusion into Gondwana coals. *Nature*, 435: 479–482.
- MCINERNEY F.A., WING S.L. 2011 – The Paleocene-Eocene thermal maximum: a perturbation of carbon cycle, climate, and biosphere with implications for the future. *Annual Review of Earth and Planetary Sciences*, 39: 489–516.
- MEISSNER K.J., BRALOWER J., ALEXANDER K., DUNKLEY T., SIPP J.W., WARD M. 2014 – The Paleocene-Eocene Thermal Maximum: how much carbon is enough? *Paleoceanography*, 29: 946–963.
- MILLS B.J.W., KRAUSE A.J., SCOTSESE C.R., HILL D.J., SHIELDS G.A., LENTON T.M. 2019 – Modelling the long-term carbon cycle, atmospheric CO<sub>2</sub>, and Earth surface temperature from late Neoproterozoic to present day. *Gondwana Research*, 67: 172–186.

- MUDELSEE M., BICKERT T., LEAR C.H., LOHMANN G. 2014 – Cenozoic climate changes: a review based on time series analysis of marine benthic  $\delta^{18}\text{O}$  records. *Reviews of Geophysics*, 52: 333–374.
- MÜLLER T., JURIKOVA H., GUTJAHR M., TOMAŠOVÝCH A., SCHLÖGL J., LIEBETRAU V.V., DUARTE L., MILOVSKÝ R., SUAN G., MATTIOLI E., PITTET B., EISENHAUER A. 2020 – Ocean acidification during the early Toarcian extinction event: evidence from boron isotopes in brachiopods. *Geology*, 48: 1184–1188.
- MURPHY B.H., FARLEY K.A., ZACHOS J.C. 2010 – An extraterrestrial  $^3\text{He}$ -based timescale for the Paleocene–Eocene thermal maximum (PETM) from Walvis Ridge, IODP Site 1266. *Geochimica et Cosmochimica Acta*, 74: 5098–5108.
- O'DONNELL J.P., NYBLADE A.A. 2014 – Antarctica's hypsometry and crustal thickness: implications for the origin of anomalous topography in East Antarctica. *Earth and Planetary Science Letters*, 388: 143–155.
- PAILARD D. 2006 – What drives the ice age cycle? *Science*, 313: 455–456.
- PARKER K.M.A., MAINELLI M.L. 2024 – What happens if we 'burn all the carbon'? carbon reserves, carbon budgets, and policy options for governments. *Environmental Science: Atmospheres*, 4: 435–454.
- PEARSON P.N., PALMER M.R. 2000 – Atmospheric carbon dioxide concentrations over the past 60 million years. *Nature*, 406: 695–699.
- PETIT J.R., JOUZEL J., RAYNAUD D., BARKOV N.I., BARNOLA J.-M., BASILE I., BENDER M., CHAPPELLAZ J., DAVIS M., DELAYGUE G., DELMOTTE M., KOTLYAKOV V.M., LEGRAND M., LIPENKOV V.Y., LORIS C., PÉPIN L., RITZ C., SALTZMAN E., STIEVENARD M. 1999 – Climate and atmospheric history of the past 420,000 years from the Vostok ice core, Antarctica. *Nature*, 399: 429–436.
- PETIT J.-R., JOUZEL J., RAYNAUD D., BARKOV N.I., BARNOLA J.-M., BASILE I., BENDER M.L., CHAPPELLAZ J.A., DAVIS M., DELAYGUE G., DELMOTTE M., KOTLYAKOV V.M., LEGRAND M., LIPENKOV V.Y., LORIS C., PÉPIN L., RITZ C., SALTZMAN E., STIEVENARD M. 2001 – Vostok – Isotope and Gas Data and Temperature Reconstruction. <https://www.ncei.noaa.gov/access/paleo-search/study/2453>. <https://doi.org/10.25921/kcxy-ae86>
- PIENKOWSKI G., HODBOD M., ULLMANN C.V. 2016 – Fungal decomposition of terrestrial organic matter accelerated Early Jurassic climate warming. *Scientific Reports*, 6, 31930.
- PIENKOWSKI G., HESSELBO S.P., BARBACKA M., LENG M.J. 2020 – Non-marine carbon-isotope stratigraphy of the Triassic–Jurassic transition in the Polish Basin and its relationships to organic carbon preservation,  $p\text{CO}_2$  and palaeotemperature. *Earth-Science Reviews*, 210, 103383.
- PIENKOWSKI G., UCHMAN A., NINARD K., PAGE K.N., HESSELBO S.P. 2024 – Early Jurassic extrinsic solar system dynamics versus intrinsic Earth processes: Toarcian sedimentation and benthic life in deep-sea contourite drift facies, Cardigan Bay Basin, UK. *Progress in Earth and Planetary Science*, 11: 18.
- PRICE G.D. 1999 – The evidence and implications of polar ice during the Mesozoic. *Earth-Science Reviews*, 48: 183–210.
- REOLID M., MATTIOLI E., DUARTE L.V., MAROK A. 2020 – The Toarcian Oceanic Anoxic Event and the Jenkyns Event (IGCP-655 final report). *Episodes*, 43: 833–844.
- REES P.M., ZIEGLER A.M., VALDES P.J. 2000 – Jurassic phytogeography and climates: new data and model comparison. [In:] Hubert B.T., Macleod K.G., Wing S.L. (eds.), *Warm Climates in Earth History*. Cambridge University Press: 297–318.
- REMÍREZ M.N., ALGEO T.J. 2020 – Carbon-cycle changes during the Toarcian (Early Jurassic) and implications for regional versus global drivers of the Toarcian oceanic anoxic event. *Earth-Science Reviews*, 209, 103263.
- RETALLACK G.J. 2002 – Carbon dioxide and climate over the past 300 Myr. *Philosophical Transactions of the Royal Society A*, 360: 659–673.
- RÖHL U., WESTERHOLD T., BRALOWER T.J., ZACHOS J.C. 2007 – On the duration of the Paleocene–Eocene thermal maximum (PETM). *Geochemistry, Geophysics, Geosystems*, 12, Q12002.
- ROYER D.L. 2006 –  $\text{CO}_2$ -forced climate threshold during the Phanerozoic. *Geochimica et Cosmochimica Acta*, 70: 5665–5675.
- ROYER D.L., BERNER R.A., MONTAÑEZ I.P., TABOR N.J., BEERLING D.J. 2004 –  $\text{CO}_2$  as a primary driver of Phanerozoic climate. *GSA Today*, 14: 4–10.
- SCHALLER M.F., FUNG M.K., WRIGHT J.D., KATZ M.E., KENT D.V. 2016 – Impact ejecta at the Paleocene–Eocene boundary. *Science*, 354: 225–229.
- SCOTÈSE C.R., SONG H., MILLS B.J.W., VAN DER MEER D.G. 2021 – Phanerozoic paleotemperatures: the earth's changing climate during the last 540 million years. *Earth-Science Reviews*, 215, 103503.
- SHACKLETON N.J. 2000 – The 100,000-year ice-age cycle identified and found to lag temperature, carbon dioxide, and orbital eccentricity. *Science*, 289: 1897–1902.
- SELLWOOD B.W., PRICE G.D. 1994 – Sedimentary facies as indicators of Mesozoic palaeoclimate. [In:] Allen J.R.L., Hoskins B.J., Sellwood B.W., Spicer R.A., Valdes P.J. (eds.), *Palaeoclimates and Their Modelling with Special Reference to the Mesozoic Era*. Chapman and Hall for the Royal Society: 17–25.
- SELLWOOD B.W., VALDES P.J. 2006 – Mesozoic climates: general circulation model and the rock record. *Sedimentary Geology*, 190: 269–287.
- STOLL H.M., PENA L.D., HERNANDEZ-ALMEIDA I., GUITIÁN J., TANNER T., PÁLIKE H. 2024 – Nonlinear increase in seawater  $^{87}\text{Sr}/^{86}\text{Sr}$  in the Oligocene to early Miocene and implications for climate-sensitive weathering. *Climate of the Past*, 20: 25–36.
- STOREY M., DUNCAN R.A., SWISHER C.C. 2007 – Paleocene–Eocene Thermal Maximum and the opening of the Northeast Atlantic. *Science*, 316: 587–589.
- SUAN G., MATTIOLI E., PITTET B., LÉCUYER C., SUCHÉRAS-MARX B., DUARTE L.V., PHILLIPPE M., REGGIANI L., MARTINEAU F. 2010 – Secular environmental precursors to Early Toarcian (Jurassic) extreme. *Earth and Planetary Science Letters*, 290: 448–458.
- SUAN G., VAN DE SCHOOTBRUGGE B., ADATTE T., FIEBIG J., OSCHMANN W. 2015 – Calibrating the magnitude of the Toarcian carbon cycle perturbation. *Paleoceanography*, 30: 495–509.
- SLUIJS A., BRINKHUIS H. 2008 – Rapid carbon injection and transient global warming during the Paleocene–Eocene thermal maximum. *Netherlands Journal of Geosciences – Geologie en Mijnbouw*, 87: 201–206.
- SVENSEN H., PLANKE S., MALTHE-SØRENSEN A., JAMTVEIT B., MYKLEBUST R., EIDEM T.R., REY S.S. 2004 – Release of methane from a volcanic basin as a mechanism for initial Eocene global warming. *Nature*, 429: 542–545.
- THEM II T.R., GILL B.C., CARUTHERS A.H., GRÖCKE D.R., TULSKY E.T., MARTINDALE R.C., POULTON T.P., SMITH P.L. 2017 – High-resolution carbon isotope records of the Toarcian Oceanic Anoxic Event (Early Jurassic) from North America and implications for the global drivers of the Toarcian carbon cycle. *Earth and Planetary Science Letters*, 459: 118–126.
- THOMAS E. 2008 – Descent into the icehouse. *Geology*, 36: 191–192.
- TURNER S.K., RIDGWELL A. 2016 – Development of a novel empirical framework for interpreting geological carbon isotope excursions, with implications for the rate of carbon injection across the PETM. *Earth and Planetary Science Letters*, 435: 1–13.
- WIERZBOWSKI H. 2013 – Strontium isotope composition of sedimentary rocks and its application to chemostratigraphy and palaeoenvironmental reconstructions. *Annales UMCS Lublin-Polonia, Section AAA*, 68: 23–37.
- WIERZBOWSKI H., ANCKIEWICZ R., PAWLAK J., ROGOV M.A., KUZNETSOV A.B. 2017 – Revised Middle–Upper Jurassic strontium isotope stratigraphy. *Chemical Geology*, 466: 239–255.
- WRIGHT J.D., SCHALLER M.F. 2013 – Evidence for a rapid release of carbon at the Paleocene–Eocene thermal maximum. *Proceedings of the National Academy of Sciences*, 110: 15908–15913.
- XU W., RUHL M., JENKYN H.C., LENG M.J., HUGGET J.M., MINISINI D., ULLMANN C.U., RIDING J.B., WEIJERS J.W.H., STORM M.S., PERCIVAL L.M.E., TOSCA N.J., IDIZ E.F., TEGELAAR E.W., HESSELBO S.P. 2018 – Evolution of the Toarcian (Early Jurassic) carbon-cycle and global climatic controls on local sedimentary processes (Cardigan Bay Basin, UK). *Earth and Planetary Science Letters*, 484: 396–411.
- ZACHOS J., PAGANI M., SLOAN L., THOMAS E., BILLUPS K. 2001 – Trends, rhythms, and aberrations in global climate 65 Ma to present. *Science*, 292: 686–693.
- ZEEBE R.E., ZACHOS J.C., DICKENS G.R. 2009 – Carbon dioxide forcing alone insufficient to explain Palaeocene–Eocene Thermal Maximum warming. *Nature Geoscience*, 2: 576–580.
- ZHANG Z.-S., YAN Q., WANG H.-J. 2010 – Has the Drake Passage played an essential role in Cenozoic cooling? *Atmospheric and Oceanic Science Letters*, 3: 288–292.
- ZHANG L., HAY W.W., WANG C., GU X. 2019 – The evolution of latitudinal temperature gradients from the latest Cretaceous through the Present. *Earth-Science Reviews*, 189: 147–158.

The work was received by the editorial office on 6.12.2024  
Accepted for printing on 30.01.2025